

# **REPORT OF THE ANS ALUMINUM CLADDING CORROSION WORKSHOP**

November 16-17, 1988  
Idaho Falls, Idaho

G. H. Hanson (Retired)  
G. W. Gibson (Retired)  
J. C. Griess (Retired)

R. E. Pawel  
*Oak Ridge National Laboratory*

N. E. Pace  
J. M. Ryskamp  
*Idaho National Engineering Laboratory*

February 1989

Prepared by the  
Oak Ridge National Laboratory  
Oak Ridge, Tennessee 37831  
Operated by  
MARTIN MARIETTA ENERGY SYSTEMS, INC.  
for the  
U.S. DEPARTMENT OF ENERGY  
under contract DE-AC05-84OR21400

**MASTER**

DISTRIBUTION OF THIS DOCUMENT IS UNLIMITED



## CONTENTS

	<u>Page</u>
LIST OF FIGURES .....	v
LIST OF TABLES .....	vii
SUMMARY .....	ix
ABSTRACT .....	1
1. INTRODUCTION .....	1
2. ANS REACTOR DESCRIPTION .....	3
3. CORROSION TESTING IN THE ANS CORROSION TEST LOOP .....	5
4. A NEW INTERPRETATION OF OXIDE FORMATION RATES AND THICKNESS LIMITS .....	9
5. EXAMINATION OF DATA TO DETERMINE TRENDS AND MECHANISMS .....	11
6. INEL FUEL CORROSION EXPERIENCE .....	13
7. ADVANCED TEST REACTOR OXIDE DATA BASE .....	15
8. RELATIONSHIP OF ALUMINUM OXIDE SOLUBILITY TO ALUMINUM CORROSION IN HIGH-TEMPERATURE DEIONIZED WATER .....	17
9. CORROSION OF ALUMINUM AT THE SAVANNAH RIVER PLANT .....	19
10. HIGH FLUX BEAM REACTOR OXIDE DATA .....	21
11. OPERATING EXPERIENCE OF THE UNIVERSITY OF MISSOURI RESEARCH REACTOR .....	23
12. SUGGESTIONS FOR ALUMINUM OXIDE RESEARCH .....	25
12.1 ANS-ORNL Corrosion Loop and Associated Research .....	25
12.1.1 Near-Term Program .....	25
12.1.2 Long-Term Program .....	25
12.2 General Aluminum Cladding Corrosion Research .....	26
12.2.1 In-Reactor Research .....	26
12.2.2 Ex-Reactor Research .....	27
REFERENCES AND BIBLIOGRAPHY .....	29
APPENDIX A. WORKSHOP PROGRAM .....	31
APPENDIX B. LIST OF ATTENDEES .....	37

## LIST OF FIGURES

<u>Figure</u>		<u>Page</u>
3.1	Measured and predicted (Griess correlation) film buildup during tests under ANS thermal-hydraulic conditions in pH-5 and pH-6 coolant water .....	6
3.2	ANS CTEST No. 3, pH=6; time histories of specimen temperature .....	7
3.3	ANS CTEST No. 4, pH=5; time histories of specimen temperatures .....	8
5.1	Measured and predicted film thickness during ANS CTEST No. 3 .....	12
6.1	Illustrative temperature-time history for an ATR fuel plate hot location thermocouple .....	14
7.1	Measured vs calculated aluminum oxide thickness for element XA004R at the end of cycle 76A-1 (first cycle) .....	16
7.2	Measured vs calculated aluminum oxide thickness for element XA006R at the end of cycle 76A-1 (first cycle) .....	16
8.1	Influence of pH on the solubility of Al <sub>2</sub> O <sub>3</sub> and its hydrates at 25°C .....	18
9.1	Moderator turbidity during 1958-1976 .....	20
10.1	Hot-edge oxide buildup on plate 18 .....	22
11.1	Oxide measurements on 775-g fuel elements .....	24

**LIST OF TABLES**

<u>Table</u>		<u>Page</u>
2.1	Design characteristics of split-core models with involute fuel .....	4
4.1	Comparison of measured oxide-film thickness with thickness predicted by Griess correlation .....	10

## SUMMARY

The Advanced Neutron Source (ANS) will be a new user experimental facility for neutron research, isotope production, and materials irradiation and will be a steady-state source of neutrons of unprecedented intensity. The ANS reactor core will probably have a configuration similar to the present Oak Ridge National Laboratory (ORNL) High Flux Isotope Reactor (HFIR). The ANS core will have an array of aluminum alloy clad fuel plates cooled by high-velocity (27.4-m/s) heavy water.

In the early 1960s, the HFIR project supported a corrosion test program that examined the behavior of several aluminum alloys under HFIR conditions. As a result of these corrosion tests and other considerations, aluminum alloy 6061 was chosen for the HFIR fuel cladding. During the past 20 years little if any research or development work has been conducted on the use of aluminum alloys for cladding of nuclear fuel plates. The higher heat flux associated with the ANS design may lead to unacceptably high local fuel temperatures and clad penetration unless the rate of oxide formation can be reduced. A pressurized-water test loop has been constructed and commissioned at ORNL to study oxide buildup on test specimens of aluminum alloy 6061 (and possibly other alloys) at ANS conditions.

An ANS Aluminum Corrosion Workshop was held at the Idaho National Engineering Laboratory (INEL) in Idaho Falls, Idaho, on November 16 and 17, 1988, to (1) develop suggestions and directions to support the experimental program for the ORNL-ANS Test Loop, (2) define gaps in current knowledge, and (3) make suggestions concerning additional research and development needed to support ANS design and operation. Initial ORNL-ANS test loop results indicate that significantly thicker oxide films than expected are encountered at the higher ANS heat flux and coolant velocity conditions. Aluminum plate temperatures above 300°C were quickly reached in these initial tests; these high temperatures and/or the associated oxide layer spalling and subsequent local corrosion may cause fuel cladding failure.

Advanced Test Reactor (ATR) and Engineering Test Reactor (ETR) operations at INEL have shown that oxide films reached limiting thicknesses and were definitely thinner (with no spalling) than expected based on the 1960s ex-reactor ORNL test loop and other data. The reason for this limit is not fully understood, but some interesting theories were offered.

Several workshop participants suggested that the reproducibility of the ANS test loop results should be checked, principally because of the suspected sensitivity of the oxidation behavior to impurity levels in the coolant. Also, the heat flux and operating limits of 6061 aluminum alloy cladding for ANS fuel plates need to be established at a coolant pH of 5.0 and at other values. If ANS requirements are not achieved, a pretreatment similar to that used for ATR fuel should be investigated. Preliminary ORNL ex-reactor results suggest that 6061 alloy may not be an acceptable cladding material for ANS fuel elements at heat fluxes much greater than  $6 \text{ MW/m}^2$  ( $2 \times 10^6 \text{ Btu/h-ft}^2$ ), unless a protective surface treatment or corrosion inhibitor is found. Alloy 6061 is supported by extensive HFIR and ATR experience, and if 6061 does not meet ANS requirements, an extensive development program will be necessary. Possible candidate alternate alloys are 8001, 2219, 5052, and 5454. A laboratory study, concurrent with loop tests with 6061, is recommended to identify alternative potentially suitable alloys.

The Workshop participants concluded that (1) currently there are inadequate experimental facilities to obtain the needed data in a timely fashion and (2) there is a very serious lack of basic understanding of the corrosion mechanisms of aluminum alloys.

## ABSTRACT

The Advanced Neutron Source (ANS) Corrosion Workshop on aluminum cladding corrosion in reactor environments is summarized. The Workshop was held to examine the aluminum cladding oxidation studies being conducted in support of the ANS design. This report was written principally to provide a record of the ideas and judgments expressed by the workshop attendees. The ANS operating heat flux is significantly higher than that in existing reactors, and early experiments indicate that there may be an aluminum cladding oxidation problem unique to higher heat fluxes or associated cladding temperatures that, if not solved, may limit the operation of the ANS to unacceptably low power levels.

A brief description of the information presented by each speaker is included along with a compilation of the most significant ideas and recommended research areas. The appendixes contain a copy of the workshop agenda and a list of attendees.

---

## 1. INTRODUCTION

An Advanced Neutron Source (ANS) Corrosion Workshop was held at the Idaho National Engineering Laboratory (INEL), Idaho Falls, Idaho, on November 16 and 17, 1988. Cochairmen were Richard E. Pawel, Oak Ridge National Laboratory (ORNL), and Norman E. Pace, INEL. The program and list of attendees are given in Appendixes A and B, respectively. The authors attempted to summarize the Workshop presentations and associated discussions. Readers for whom this record is inadequate are invited to contact INEL (N. E. Pace or J. M. Ryskamp) or ORNL (R. E. Pawel) to obtain further information.

The ANS Corrosion Workshop was held to (1) review the established corrosion and oxidation behavior on aluminum-clad fuel elements in high-performance reactors and (2) assess the preliminary results from the ANS experimental program. The Workshop helped to identify gaps in the data base where information is needed to predict the behavior of aluminum cladding on ANS fuel elements; in addition, it provided information helpful in formulating the experimental program and other work needed to define the corrosion of aluminum cladding.

The corrosion-product film on water-cooled aluminum fuel plates is chiefly a mixture of alumina hydrates. Two alumina hydrates are commonly found on aluminum exposed to water, the monohydrate and the trihydrate. There are two crystalline forms of each hydrate: the monohydrates — boehmite and diasporite — and the trihydrates — bayerite and gibbsite. Bayerite is not found in nature. The crystalline forms found on reactor fuel plates are chiefly the low-temperature form, bayerite, and the higher-temperature form, boehmite. The ex-reactor transition temperature from bayerite to boehmite is  $\sim 80^{\circ}\text{C}$ . Indications of amorphous alumina have been found on aluminum-clad fuel plates that have been irradiated.

The next section describes the ANS reactor. Sections 3 through 11 are brief summaries of each of the presentations given at the Workshop. Section 12 presents some suggestions for future research that would help define the corrosion and oxidation characteristics important to ANS operation.



## 2. ANS REACTOR DESCRIPTION

A high-performance reactor producing ultrahigh neutron fluxes and designated the Advanced Neutron Source (ANS) is being designed to reestablish the United States as the leader in research on neutron interactions with matter. The ANS, which is scheduled to begin operation in 1998, will be used for basic physics and materials research and also for the production of radioisotopes. This is a very important project because all reactors with high enough fluxes to conduct such experiments were built in the 1960s and are approaching the end of their predicted lifetimes.

An axially split-core reactor with involute fuel plates has been proposed for the ANS. A close-in core pressure boundary tube (CPBT) separates the core and its coolant from the low-temperature, low-pressure pool environment for the experimental sources and beams. The ANS split core incorporates several features that qualify it for this specific application. These features include the capability to produce thermal-neutron-flux levels 5 to 10 times higher than those in current research reactors, a hospitable environment for the neutron-beam tubes and cold/hot sources, and flexible beam access arrangements. The core consists of two halves cooled by heavy water. The halves are separated by a central coolant plenum. The fuel plates are highly enriched uranium silicide in an aluminum matrix clad with aluminum alloy. The thermal-neutron flux peaks outside of the CPBT in a large tank of heavy water. Design characteristics of split-core models are given in Table 2.1.

The reactor must have a high power density to produce neutrons efficiently at the desired flux levels. Therefore, the thin fuel plates have a very high heat flux across the aluminum cladding and are cooled by rapidly flowing heavy water. The high thermal conductivity of the aluminum alloy cladding combines with the high heat transfer coefficient governing heat flow from the fuel plates to the water to keep the fuel inside the plates at an acceptable temperature. Unfortunately, the exposure of aluminum under these conditions leads to the formation of a thin layer of aluminum oxide that separates the fuel plates from the coolant water. Aluminum oxide has very poor thermal conductivity, which leads to increasing fuel plate temperatures as the oxide thickens. The Workshop addressed the characteristics of oxide buildup on aluminum surfaces under heat transfer conditions. These characteristics must be quantitatively described for the extremely aggressive conditions expected for the ANS reactor.

Table 2.1. Design characteristics of split-core models with involute fuel

Core volume, L	35-41
6061-Al core pressure boundary tube thickness, mm	15-30
Fuel material	U <sub>3</sub> Si <sub>2</sub> /Al
Uranium enrichment, wt % <sup>235</sup> U	93
Maximum fuel density, kg U/L fuel meat	4.8
Fuel plate thickness, mm	1.27
Coolant channel width, mm	1.27
Fuel meat thickness, mm	0.762
Cladding and side plate material	6061-Al
Cladding thickness, mm	0.254
Fuel volume fraction in core	0.3
Coolant volume fraction in core	0.5
6061-Al volume fraction in core	0.2
Reactor power (constant), MW(t)	300-350
Cycle length, days at full power	14.0 (or greater)
Core average power density, MW(t)/L	6.5-8.5
Peak reflector thermal-neutron flux, E < 0.625 eV, neutrons/(m <sup>2</sup> ·s)	7-9 × 10 <sup>19</sup>
Core fissile loading at BOC, kg <sup>235</sup> U	20-30
Fuel burnup, kg <sup>235</sup> U	5-6
Peak fissions/m <sup>3</sup> meat	1-2 × 10 <sup>27</sup>
Average fissions/m <sup>3</sup> meat	0.8-1.0 × 10 <sup>26</sup>
Coolant velocity, m/s	27.4
Coolant inlet temperature, °C	49.0
Average channel outlet temperature, °C	<100.0
Reflector pool temperature, °C	27.0
Coolant inlet pressure, MPa	4-4.5
Average surface heat flux, MW(t)/m <sup>2</sup>	8-10
Peak surface heat flux, MW(t)/m <sup>2</sup>	12-16
Average power density in fuel meat, MW-fuel/L	20-25
Peak hot fuel plate temperature, °C	280-360

### 3. CORROSION TESTING IN THE ANS CORROSION TEST LOOP

(R. E. Pawel, G. L. Yoder, and B. H. Montgomery  
Oak Ridge National Laboratory)

In support of the ANS reactor core design, ORNL has designed and constructed a corrosion loop to study the rate of oxide-film formation under the proposed ANS operating conditions. This facility is based on the ORNL corrosion loop experience of J. C. Griess and coworkers, which supported the designs of the ORNL High Flux isotope Reactor (HFIR) and the INEL Advanced Test Reactor (ATR). The loop is designed to measure the rate of temperature increase due to oxide buildup on a reacting aluminum surface exposed to rapidly flowing water (up to 35 m/s) under high heat flux conditions (up to 20 MW/m<sup>2</sup>). The loop was completed in January 1988, and initial experimental results have already been obtained.

Illustrative experimental data (CTESTS Nos. 3 and 4) are presented in Fig. 3.1. With ANS operating conditions and the water in the test loop having a pH of 6 (CTEST 3), a midsection oxide film of 25  $\mu\text{m}$  (1 mil) was formed in 50 hours; with a pH of 5 (CTEST 4) a 25- $\mu\text{m}$  oxide film developed in 85 hours. The pH in the test loop as well as that in HFIR is controlled by small additions of nitric acid. Two sets of calculated curves based on the Griess correlation (developed from data generated at ATR and HFIR operating conditions) are also presented. These calculated curves, when compared with CTEST Nos. 3 and 4, emphasize that significantly thicker than expected oxide films are generated at the higher ANS heat flux and coolant velocity conditions. In the case of two pairs of calculated comparative curves, the lower curves for each assume zero initial oxide, and the upper curves assume the presence of a thin initial oxide layer.

During these initial tests, temperature increases on the specimen above 100°C were observed due to the buildup of oxide on the heat transfer surface, as shown in Figs. 3.2 and 3.3. This additional source of temperature increase is of concern to the integrity of the ANS fuel plates. Consequently, the need is urgent to provide a coolant environment for the ANS fuel plates that results in a very low rate of oxide formation.

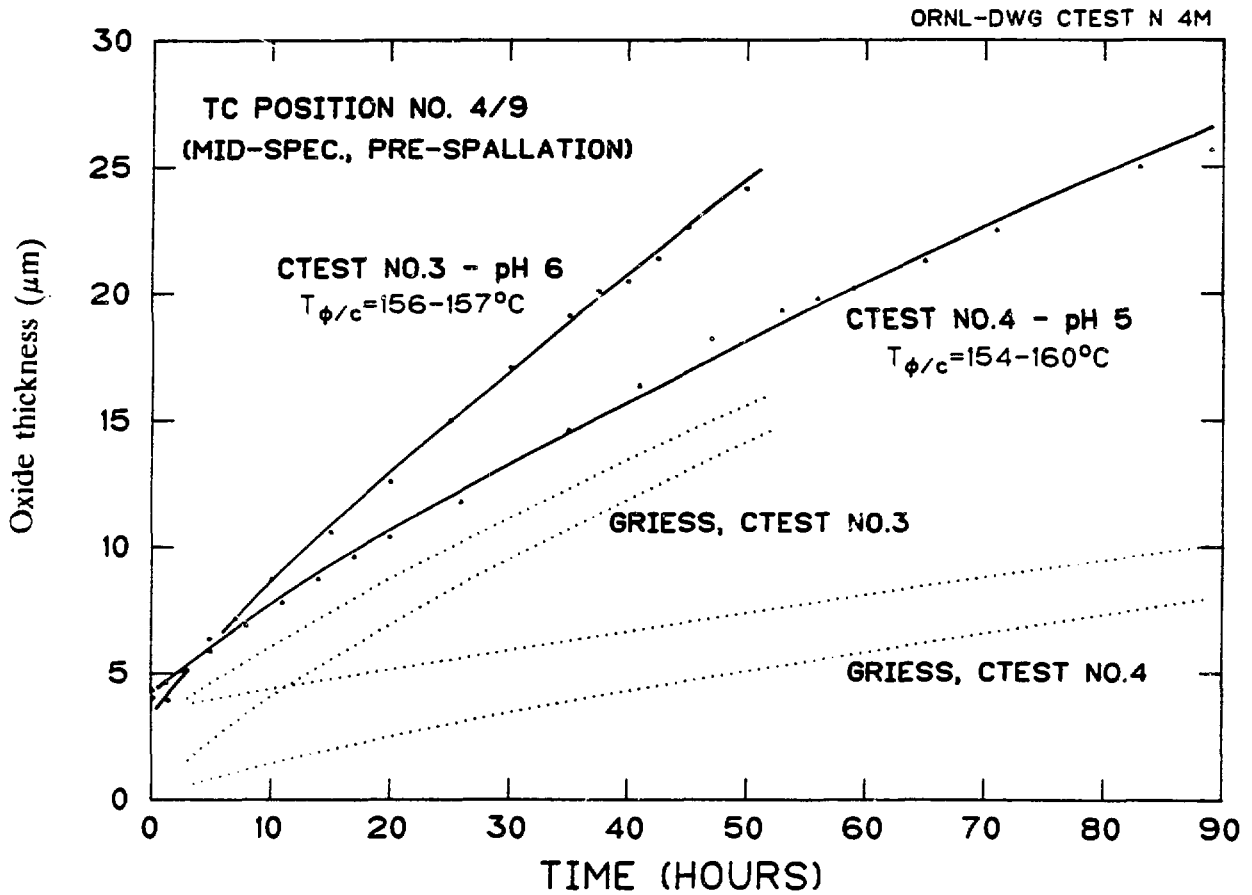


Fig. 3.1. Measured and predicted (Griess correlation) film buildup during tests under ANS thermal-hydraulic conditions in pH 5 and pH 6 coolant water.

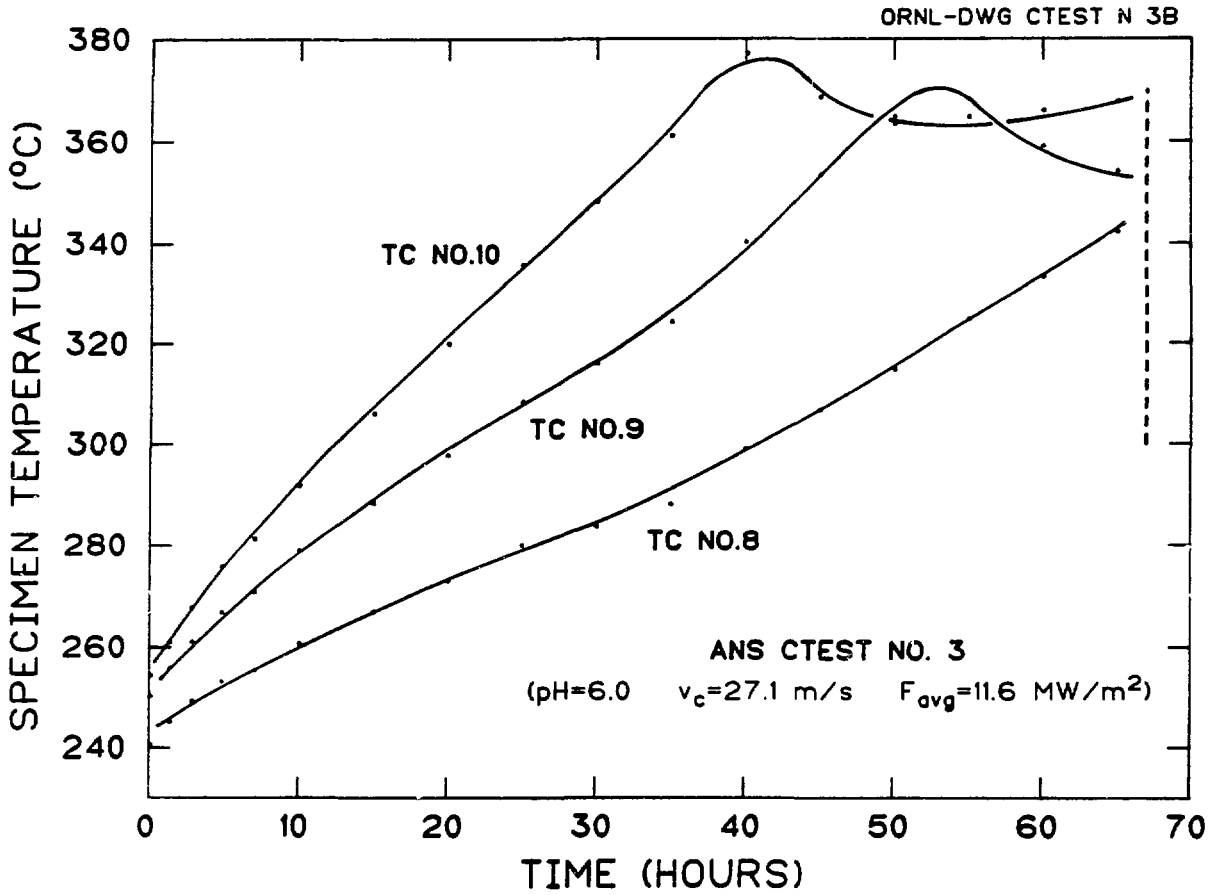


Fig. 3.2. ANS CTEST No. 3, pH=6; time histories of specimen temperatures.

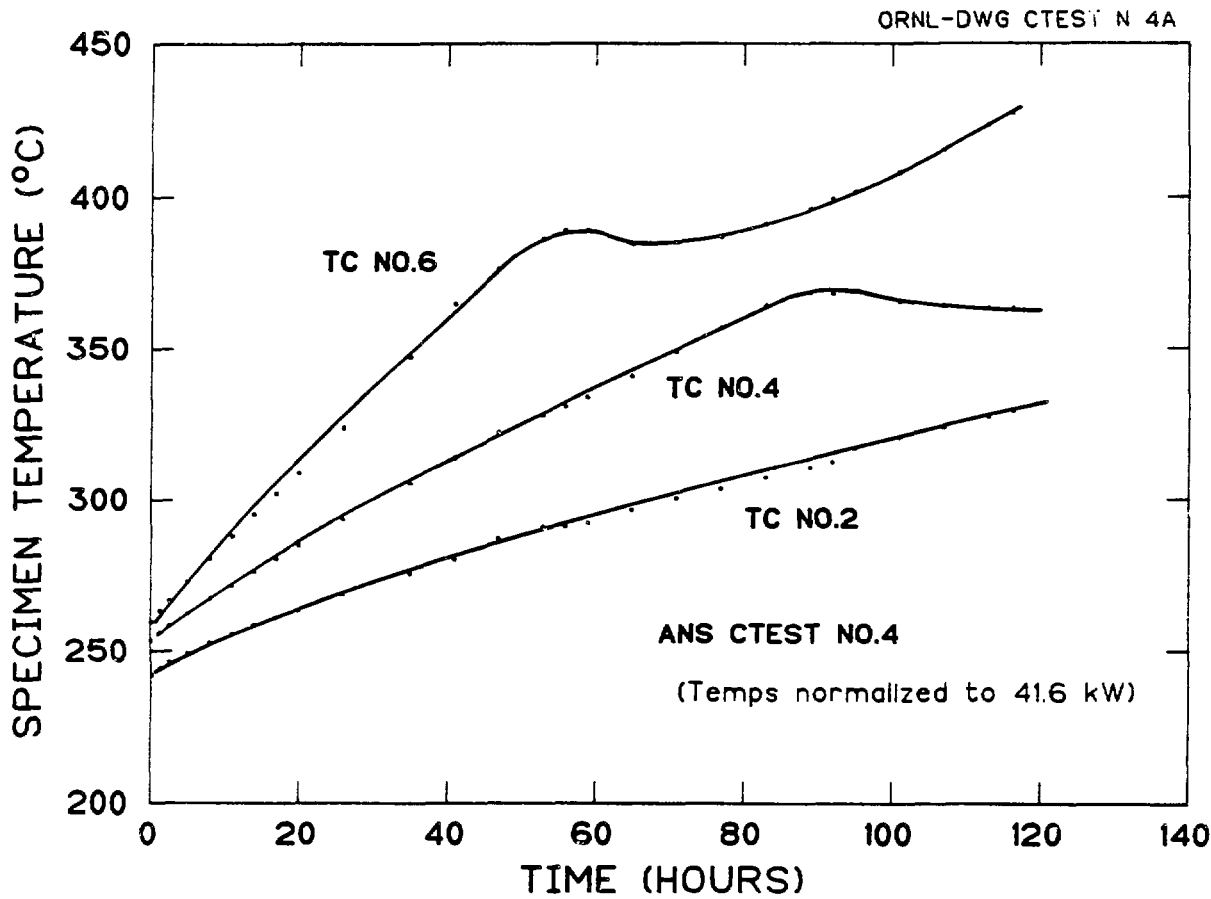


Fig. 3.3. ANS CTEST No. 4, pH=5; time histories of specimen temperature.

## 4. A NEW INTERPRETATION OF OXIDE FORMATION RATES AND THICKNESS LIMITS

(W. R. Gambill, Ideas presented by G. L. Yoder  
Oak Ridge National Laboratory)

In the early 1960s, J. C. Griess and coworkers (ORNL) developed a correlation for oxide buildup on 6061-Al alloy based on extensive ORNL ex-reactor studies at operating conditions in the range of those of INEL-ATR and ORNL-HFIR:  $H_2O$  at velocity = 7.6-15.2 m/s, coolant bulk temperature = 54-121°C, and heat flux = 3.2-6.3 MW/m<sup>2</sup>. Table 4.1 presents [ $\delta_{ox}/(\delta_{ox} \text{ Griess})$ ] ratios from data for five cases, three in-reactor and two ex-reactor;  $\delta_{ox}$  represents the measured oxide buildup, and ( $\delta_{ox} \text{ Griess}$ ) is the calculated oxide thickness based on the Griess correlation. The ratios vary from a small 0.2 to as large as perhaps 3.0. The important point is that the ratio of the maximum-to-minimum values of  $\delta_{ox}/(\delta_{ox} \text{ Griess})$  is in the range of 10 to 15, immensely larger than any experimental data scatter. These ratios indicate that a variable is missing or incompletely represented in the Griess correlation; they point to heat flux as an important variable, at least outside of the heat flux range for which the correlation was established.

This presentation also addressed the subject of oxide spallation. Oxide began spalling with a measured oxide thickness of ~75  $\mu\text{m}$  at the Savannah River Plant (SRP), ~50  $\mu\text{m}$  under ex-reactor HFIR test conditions, and ~25  $\mu\text{m}$  for ANS test conditions where the heat fluxes between reactors were in the ratio of approximately 1:2:3, respectively. These data indicate an average oxide temperature drop ( $\Delta T$ ) at spallation of about 134°C. When the  $\Delta T$  across the oxide film is 134°C, the thermal stress at the cooler surface of the oxide film is within  $\pm 15\%$  of the mean and high values of the tensile strength of alumina forms. Tentative conclusions are: (1) spallation occurs when the thermal stress in the oxide reaches its ultimate tensile strength and (2) while there is not a critical oxide thickness, there is a critical oxide  $\Delta T$  of 130-140°C.

Table 4.1. Comparison of measured oxide-film thickness with thickness predicted by Griess correlation

Case No.	Reactor	Years	Coolant	$\sim\theta$ (d)	V (m/s)	$\sim\theta_{max}$ (MW/m <sup>2</sup> )	$\phi/V$ (MWs/m <sup>3</sup> )	$\phi/V$ (MW/ms)	$\frac{\delta_{ox}}{(\delta_{ox})_{Griess}}$ <sup>a</sup>
1	SRP (production) <sup>b</sup>	76-77	D <sub>2</sub> O	270	5.8	2.2	0.38	12.8	0.2
2	ATR <sup>c</sup>	~87	H <sub>2</sub> O	80-100 (max)	13.7	<5; 4(avg)	0.29	54.8	0.7
3	HFIR (c. tests)	Early 60s	H <sub>2</sub> O	20 (max)	15.2 (max)	6.3	0.41	95.8	1.0 <sup>d</sup>
4	HFIR [100 MW(t)]	Through 11/86	H <sub>2</sub> O	23	16.2	6.2	0.38	100.4	1.0 <sup>e</sup>
5	ANSR (c. test 4) <sup>f</sup>	88	H <sub>2</sub> O	5	27.4	12.0	0.44	328.8	2.0-3.0; 2.7?
6	ANSR (design)	88	D <sub>2</sub> O	14-15	27.4	17.0	0.62	465.8	3?

<sup>a</sup>For coolant pH ≈ 5.0.

<sup>b</sup>Oxide thickness ratio from R. S. Ondrejcin, SRL Memo DPST-83-324, p. 4, March 1983.

Operating conditions from DPSTSA-100-1, deleted version, p. 4-44 (Rev. January 1981).

<sup>c</sup>For ATR oxide data base being reevaluated by INEL reactor power <190 MW(t); average power ≈150 MW(t).

<sup>d</sup>± ~25%.

<sup>e</sup>Presumed; no oxide data obtained shortly after shutdown are available.

<sup>f</sup>Oxide thickness ratio from G. L. Yoder and R. E. Pawel, telephone conversation of Sept. 15-20, 1988.



## 5. EXAMINATION OF DATA TO DETERMINE TRENDS AND MECHANISMS

(G. L. Yoder, Oak Ridge National Laboratory)

A detailed thermal analysis of the specimen used during ANS CTEST No. 3 was made using the two-dimensional conduction code CONDUCT. CONDUCT has the following features:

Finite difference formulation  
Examines axial slices along heated length  
Allows redistribution of power  
Oxide growth included

Assumptions:

- steady state
- constant voltage drop per unit axial length
- Griess temperature/time relationships are valid
- Petukhov heat transfer coefficient
- insulated boundaries where no water is present

The top portion of Fig. 5.1 gives a diagram of the calculational model of a quarter of the corrosion test specimen. The bottom portion shows calculated curves of oxide thickness in a slice of the specimen at thermocouple position 2 for 20-hour intervals up to 60 hours, which is the approximate duration of CTEST No. 3. The oxide thickness in the tab region is markedly lower than the rest of the specimen because temperatures in the tab regions are much lower. The end-of-life measured oxide values for the slice at thermocouple position 2 (the location of the hottest surface temperature) are included in Fig. 5.1. The predicted oxide thickness at the specimen centerline was forced to equal the measured value at the end of CTEST No. 3. The measured values reflect the shape of the calculated curve. The agreement between the calculated and measured specimen temperatures was good using a multiplier of 2.25 with the Griess correlation. The magnitude of this multiplier, or a better buildup correlation, still remains to be developed and verified. It is obvious, however, that the oxide growth rates in these tests imply serious limitations to the use of 6061 aluminum for fuel plates for the extremely high heat flux conditions of the ANS, if the same oxide growth rates exist in it. Detailed thermal analysis of the ORNL test section may help provide additional oxide formation characteristics.

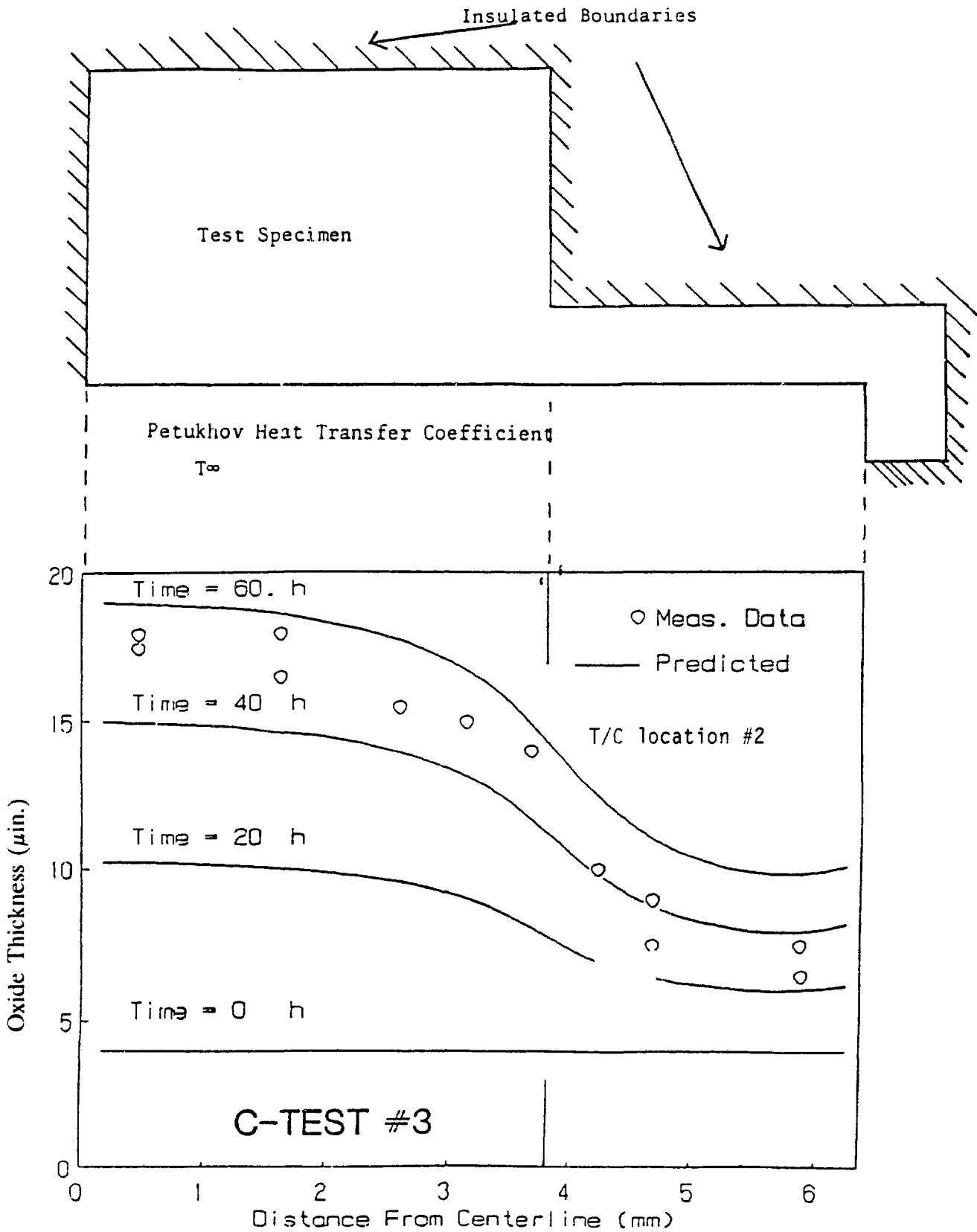


Fig. 5.1. Measured and predicted film thicknesses during ANS CTEST No. 3.

## 6. INEL FUEL CORROSION EXPERIENCE

(M. L. Griebenow and G. N. Fillmore  
Idaho National Engineering Laboratory)

The potential major fuel assembly problem for the Advanced Test Reactor (ATR) and Engineering Test Reactor (ETR) resulting from fuel plate cladding corrosion was structural failure due to overheating of the fuel plates. Another important potential problem was clad removal and fission-product release due to oxidation/spallation and corrosion. The problem-definition tasks and problem-resolution approaches were reviewed, and the major findings were discussed. No ATR fuel assembly structural problems are encountered currently provided (1) ATR uses graded fuel in high-power positions, (2) the fuel assemblies are swaged by qualified procedures (this provides sideplate-fuel plate slippage, (3) the ATR fuel elements have a thin boehmite prefilm, (4) a coolant pH near 5.0 is maintained during operation and shutdown, and (5)  $\text{Al}_2\text{O}_3 \cdot \text{XH}_2\text{O}$  in the primary coolant (dissolved and suspended) is within specifications at startup and during operation.

During ATR commissioning, a number of startup tests were performed, including a fuel-cladding oxide-buildup test. An illustrative temperature-time history for a hot location is given in Fig. 6.1. During this 8-day test the fuel plate temperature at this hot location (thermocouple position 9) increased about  $20^\circ\text{C}$  ( $35^\circ\text{F}$ ), from about  $182$  to  $202^\circ\text{C}$  ( $360$  to  $395^\circ\text{F}$ ). The temperature increase was modest compared with the ANS situation. A MACABRE-calculated temperature-time history, using the Griess correlation with a 0.7 multiplier and the Griess oxide thermal conductivity of  $2.25 \text{ W/m}\cdot^\circ\text{C}$  ( $1.3 \text{ Btu/h}\cdot\text{ft}\cdot^\circ\text{F}$ ), produced the prediction shown in Fig. 6.1. Good agreement was obtained between measured and calculated values.

At normal operating conditions, amorphous aluminum oxide and bayerite form on both ETR and ATR fuel plates, even at temperatures that would result in the formation of boehmite out of reactor. Pseudoboehmite was also detected following ATR operation, which resulted in relatively thick oxide formation (~1 mil). Distinctive oxide bilayers were observed in metallographic evaluations, indicating that the temperature of the oxide exceeded the transition temperature. The thickness of oxide that formed on fuel plates in both the ETR and the ATR is limited. The limiting thicknesses are about  $15 \mu\text{m}$  (0.6 mil) for the ATR and  $20 \mu\text{m}$  (0.8 mil) for the ETR.

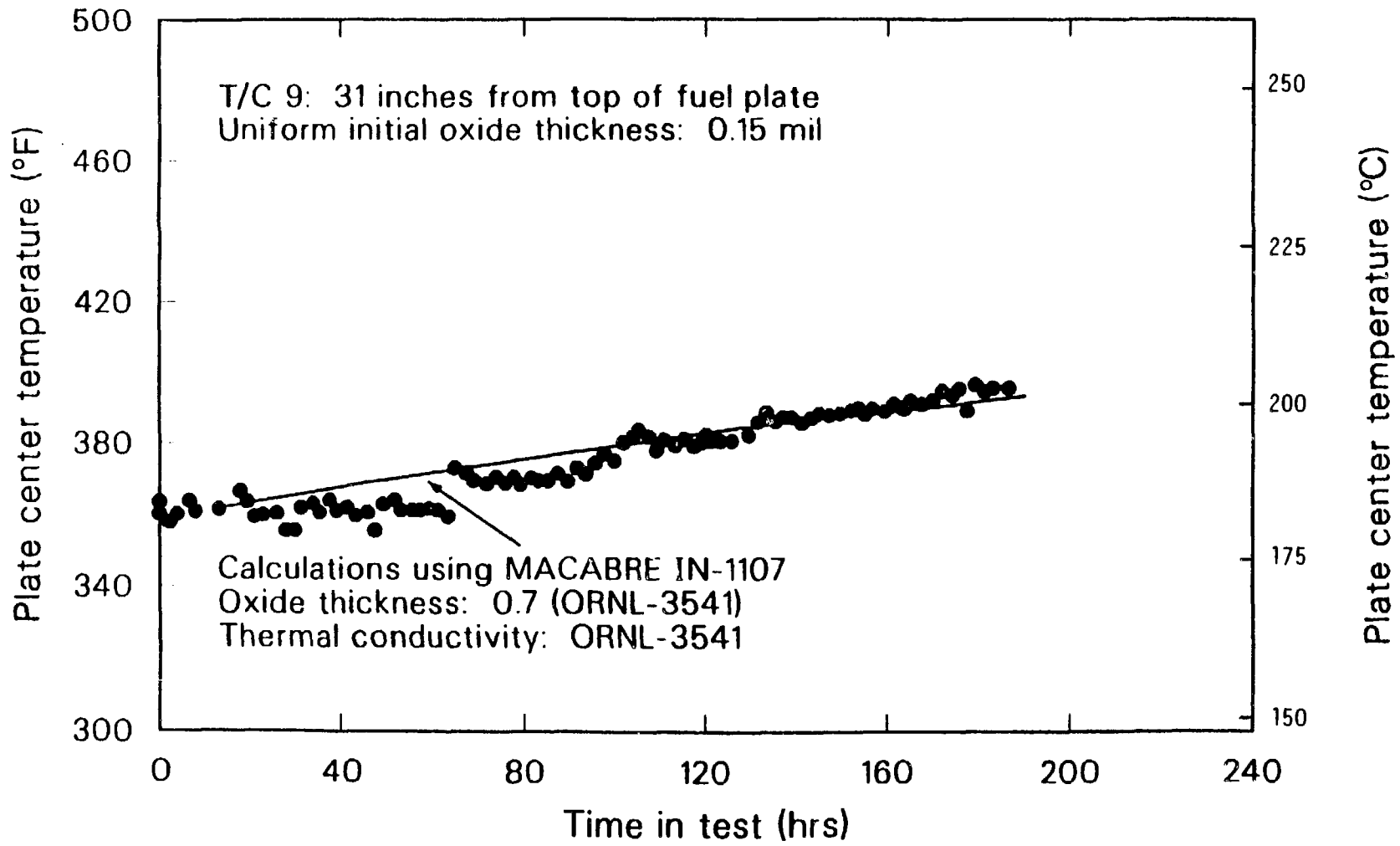


Fig. 6.1. Illustrative temperature-time history for an ATR fuel plate hot location (thermocouple 9).

## 7. ADVANCED TEST REACTOR OXIDE DATA BASE

(N. E. Pace, Idaho National Engineering Laboratory)

After each ATR operating cycle, oxide measurements are made along the hot stripe on the exterior surface of the outside fuel plate (plate 19) of one or more fuel assemblies that were operated in the hotter ATR locations. This presentation discussed the preparation of a data base of oxide measurements from the first operating cycle of 20 selected fuel assemblies. This data base is intended not only for studies by INEL investigators but also by investigators at other laboratories who are working on correlations to describe the growth of oxide films on aluminum-clad fuel plates.

The ATR plate 19 oxide measurements constitute a valuable inventory of data. However, knowledge of the thickness of the associated coolant channel is weak, because the outside wall of the channel is a beryllium structural member, which has "large" dimensional tolerances. The water temperature in the outer channel is cooler than the water temperature in the inner channels. To illustrate the effect on calculated oxide formation due to flow channel thickness uncertainty, Figs. 7.1 and 7.2 show calculated oxide thicknesses along the hot stripe (solid curves and dot-dash curves) based on the Griess correlation times a multiplier using minimum and maximum channel thicknesses, respectively. (The multiplier used with the Griess correlation was 0.5, but the calculations also included some hot channel factors; therefore, the effective multiplier is somewhat unknown for those calculations.) The maximum calculated oxide thickness uncertainty (Fig. 7.2, 0.92 m down from the top of the fuel plate) is 3.5  $\mu\text{m}$  (0.14 mils). The measured oxide thicknesses are included in these graphs using the asterisk symbol.

The maximum coolant channel has more coolant flowing down it than does the minimum channel because the velocity remains about the same. Therefore, the coolant temperature for the maximum channel is lower than for the minimum channel, and as a result of the cooler coolant temperature, the predicted oxide thickness is less for the maximum channel than it is for the minimum channel.

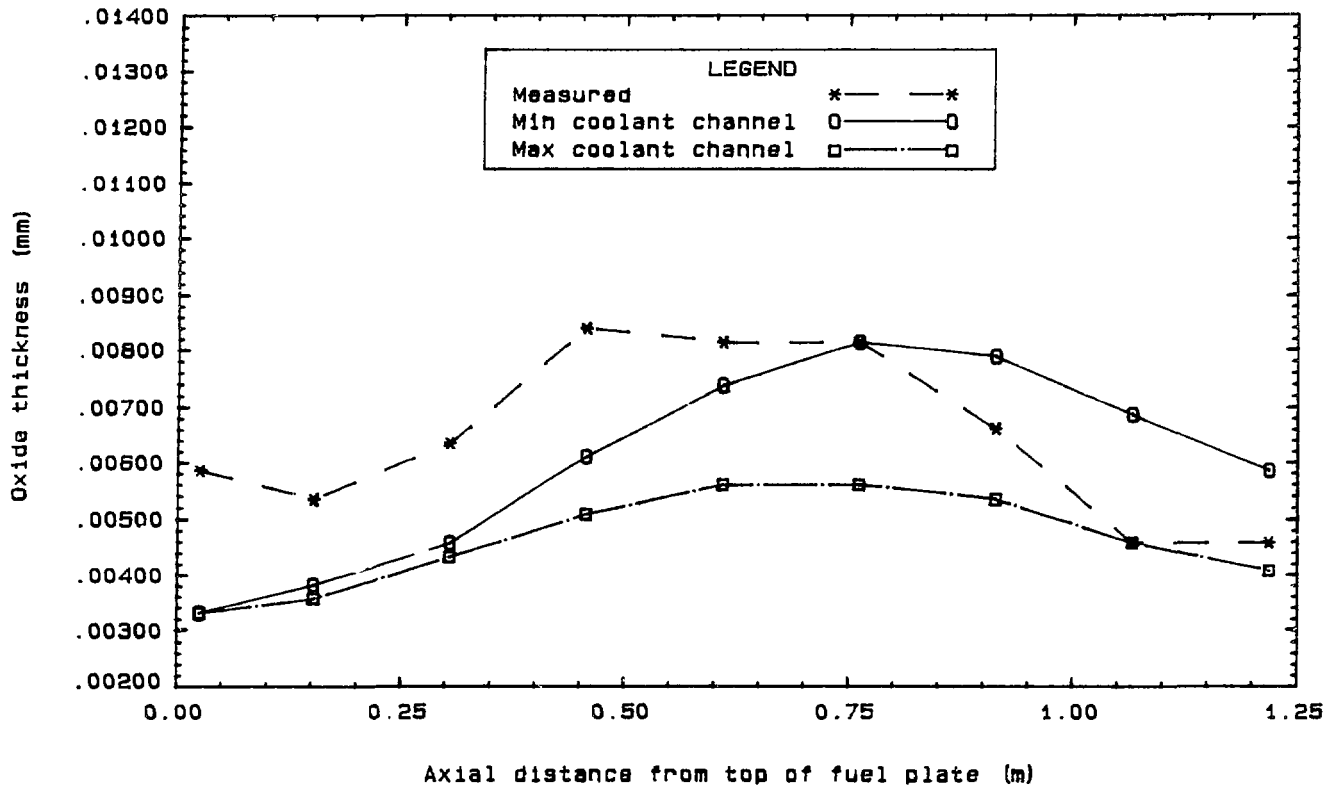


Fig. 7.1 Measured vs calculated aluminum oxide thickness for element XA004R at the end of cycle 76A-1 (first cycle).

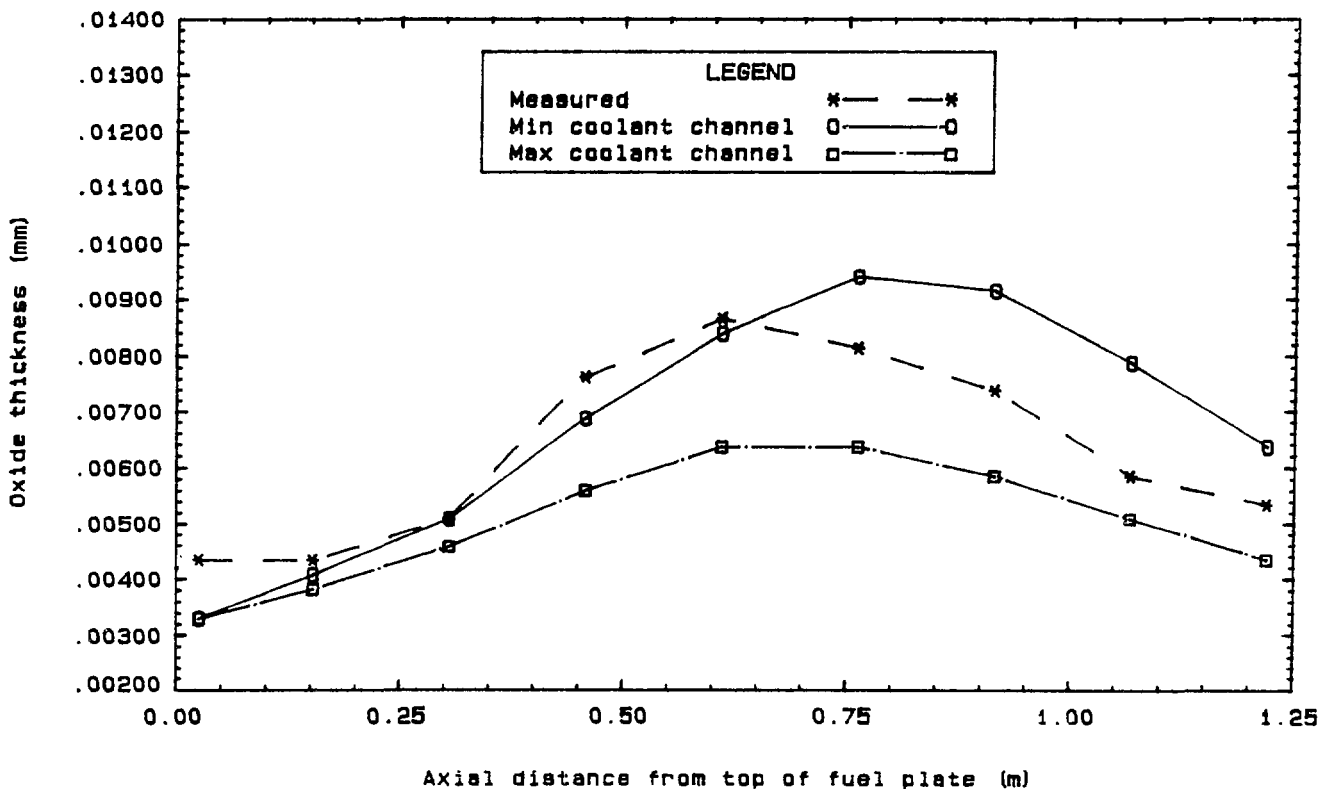


Fig. 7.2 Measured vs calculated aluminum oxide thickness for element XA006R at the end of cycle 76A-1 (first cycle).

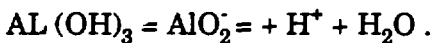
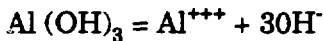
## 8. RELATIONSHIP OF ALUMINUM OXIDE SOLUBILITY TO ALUMINUM CORROSION IN HIGH-TEMPERATURE DEIONIZED WATER

(R. L. Dillon, Pacific Northwest Laboratories, Retired)

The author proposed that the variations in the reported corrosion rates from dynamic test facilities at various sites operating at the same temperature and flow rate were caused by an aluminum oxide dissolution process in the water. Measurements of oxide solubilities were made, and it was shown that corrosion rates could be predicted from oxide solubilities combined with a consideration of the removal of aluminum from the bulk water.

The aluminum corrosion product found on corroding aluminum or deposited on the other system components is a complex material consisting of a variety of oxides and hydrates. The aluminum corrosion product at 20°C consists of an amorphous oxide at the metal-oxide surface and is progressively hydrated to boehmite ( $\alpha\text{Al}_2\text{O}_3 \cdot \text{H}_2\text{O}$ ) and then to bayerite ( $\beta 3\text{Al}_2\text{O}_3 \cdot 3\text{H}_2\text{O}$ ) at the oxide-water surface. Figure 8.1 shows the solubilities at 25°C of various hydrated and nonhydrated aluminum oxides as a function of pH, as calculated from thermodynamic and electrochemical considerations. All of these oxides and hydrates have varying degrees of solubility, and the solubility varies with the pH of the coolant.

Aluminum oxides are amphoteric and may dissociate depending on the pH of the solution according to the following equations:



At low pH the  $\text{Al}^{3+}$  ion predominates, and at high pH the  $\text{AlO}_2^-$  dominates. The predominant ion is indicated by the areas to the left or to the right of the dotted vertical line in Fig. 8.1. An area of minimum solubility occurs near pH 5 at 25°C. This point of minimum solubility shifts to lower pH values as the temperature is increased. The oxides undergo a continuous aging process at room temperature through intermediate hydrates to the most stable hydrate, hydrargillite or gibbsite, which is the least soluble form. It is not clear which constituent predominates in the dissolution process. The corrosion product solubility measured by the author (marked Solubility Al corrosion product in Fig. 8.1) falls near the unhydrated aluminum oxide curve. It was concluded that the soluble species in the corrosion product film was anhydrous alumina.

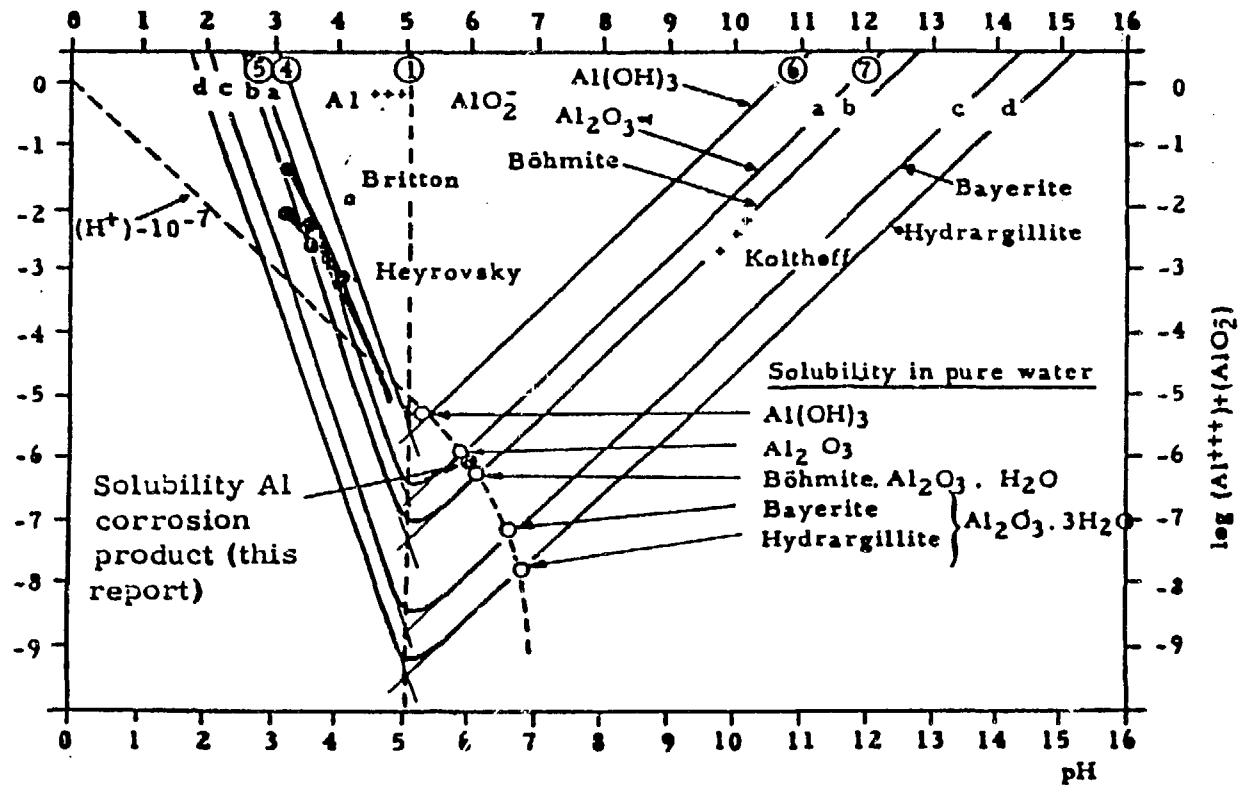


Fig. 8.1. Influence of pH on the solubility of  $Al_2O_3$  and its hydrates at 25°C.

Source: Ref. 12.



## 9. CORROSION OF ALUMINUM AT THE SAVANNAH RIVER PLANT

(R. S. Ondrejcin, Savannah River Plant)

Prior to 1963, type-1100 aluminum cladding was used for the Savannah River Plant (SRP) production reactors. Since 1963, type-8001 aluminum alloy has been used. The importance of good chemistry control for the D<sub>2</sub>O coolant and moderator was emphasized. This requirement is illustrated in Fig. 9.1, which gives the 1958-1976 history of moderator turbidity. Prior to 1960, conductivity, but not pD, was controlled. In 1960 good pD control of  $4.7 \pm 0.1$  with HNO<sub>3</sub> was also instituted, and moderator turbidity was <10 ppm, the limit at which reasonable visibility is obtained. (Note: pD control was interrupted during the very high flux operations of 1970 for the production of <sup>252</sup>Cf.)

The SRP equation for oxide buildup on cladding is the Kritz correlation:

$$C = 17.3 (Q/A)(\theta)^{0.778} \exp(-1880/K),$$

where

- C = oxide thickness, mils.
- Q/A = heat flux in  $1.8 \times 10^6$  Btu/h-ft<sup>2</sup> units,
- $\theta$  = oxide growth period, d,
- K = absolute temperature, K, at the oxide-water interface.

The Kritz equation is similar to the Griess equation, except that it explicitly includes heat flux as a variable. The kinetic form is identical, with the rate-determining temperature also assigned to that of the oxide-coolant interface. However, a different activation energy is utilized.

Ondrejcin discussed black aluminum oxide. A study in 1980 revealed that the oxide at the top of Savannah River tubes was white gibbsite,  $\alpha\text{Al}_2\text{O}_3 \cdot 3\text{D}_2\text{O}$ ; the oxide on the bottom two-thirds of the tubes was black boehmite,  $\alpha\text{Al}_2\text{O}_3 \cdot \text{D}_2\text{O}$ . The black color was due to either tiny aluminum particles (<100 Å in diameter) or F centers (crystal lattice defects).

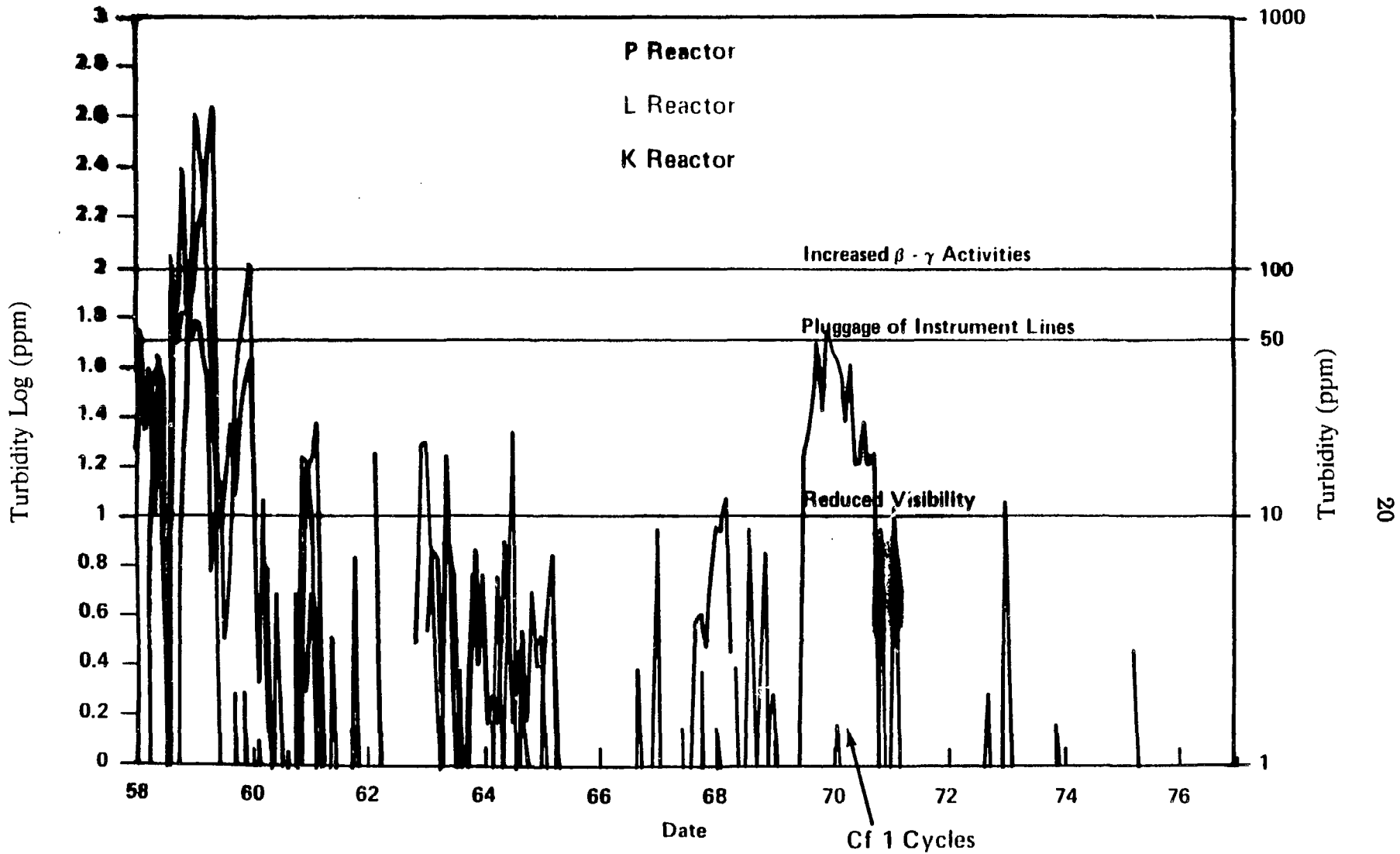


Fig. 9.1. Moderator turbidity during 1958-1976.

## 10. HIGH FLUX BEAM REACTOR OXIDE DATA

(J. Weeks, Brookhaven National Laboratory)

Measurements of oxide buildup on irradiated fuel elements were performed by INEL personnel during the July 1971 shutdown of the High Flux Beam Reactor (HFBR) at Brookhaven National Laboratory. The elements examined included those that had been discharged during the July shutdown and others discharged earlier. All of the elements had been irradiated routinely for approximately two 20-day cycles at full reactor power. Individual fuel plates were removed from the elements by breaking the swaged joint between the side plate and the fuel plate. All of the data for the hot edges of plate 18 of elements discharged from position C-6 and the equivalent C-12 position are presented in Fig. 10.1.

There does not appear to be a noticeable difference between the data obtained from recently discharged and old elements (that have been stored in water for some time), and both sets of data were included. One unexpected feature of the data was that the oxide on the convex side of the plate tended to be thicker than on the concave side. The solid curve in Fig. 10.1 represents the "average" oxide thickness along the hot edge of fuel plate 18; the dashed lines represent the predicted values of oxide buildup at the end of a typical equilibrium cycle, using the Griess correlation and the MACABRE calculated fuel plate temperature. The lower dashed curve is based on nominal conditions, and the upper curve reflects the 2 sigma or 97.5% confidence limits on the hot channel parameters. The agreement between experiment and prediction is only fair. However, the 2 sigma curves for both plates 18 and 19 yield conservative estimates of the oxide buildup as compared with the measured data.

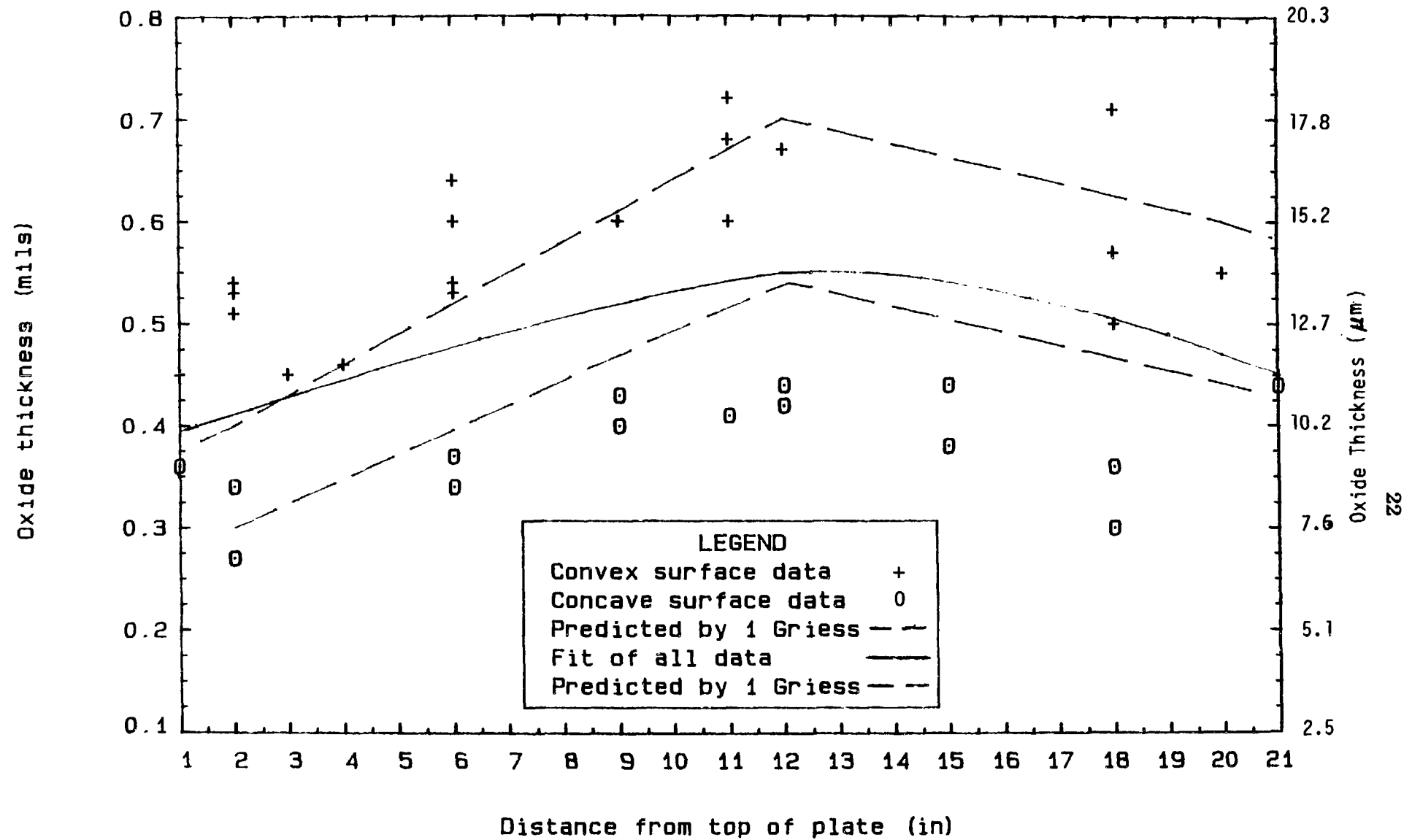


Fig. 10.1. Hot-edge oxide buildup on plate 18. Element from HFBR core positions C-6 and C-12.

## 11. OPERATING EXPERIENCE OF THE UNIVERSITY OF MISSOURI RESEARCH REACTOR

(J. Charles McKibben, University of Missouri-Columbia)

The University of Missouri Research Reactor (MURR) upgrade was discussed, focusing on the new fuel design for the increased reactor power and fuel element life. The MURR fuel element is of the ATR type, but with 24 fuel plates. The new fuel design is supported by a successful run in ATR with peak burnup of  $3 \times 10^{27}$  fissions/m<sup>3</sup>. UAl<sub>2</sub> is the primary fuel constituent and provides a fuel density of  $3.0 \times 10^3$  kg U/m<sup>3</sup> when 50 vol % UAl<sub>x</sub> powder is used. The two new fuel element designs consist of a 1.270-kg fuel element using untapered fuel and a 1.244-kg fuel element using tapered fuel.

The maximum oxide thickness measurements on plate 24 for 17 old style fuel elements are given in Fig. 11.1 as a function of power history presented as (megawatt days)<sup>0.778</sup>. The data points with an asterisk were not used for the regression fit. These fuel elements were in their first cycle when the coolant pH was out of control due to resin failure. The other fuel elements were either in their second or greater cycle and were not affected adversely by poor water chemistry because of their oxide prefilm. The MURR equation for oxide growth is

$$\Delta X = 0.009612 (\text{MWD})^{0.778}; \Delta X \text{ is in mils .}$$

For general oxide calculations, the MURR staff uses the Griess correlation with a 0.7 multiplier.

● experimental points

— regression fit

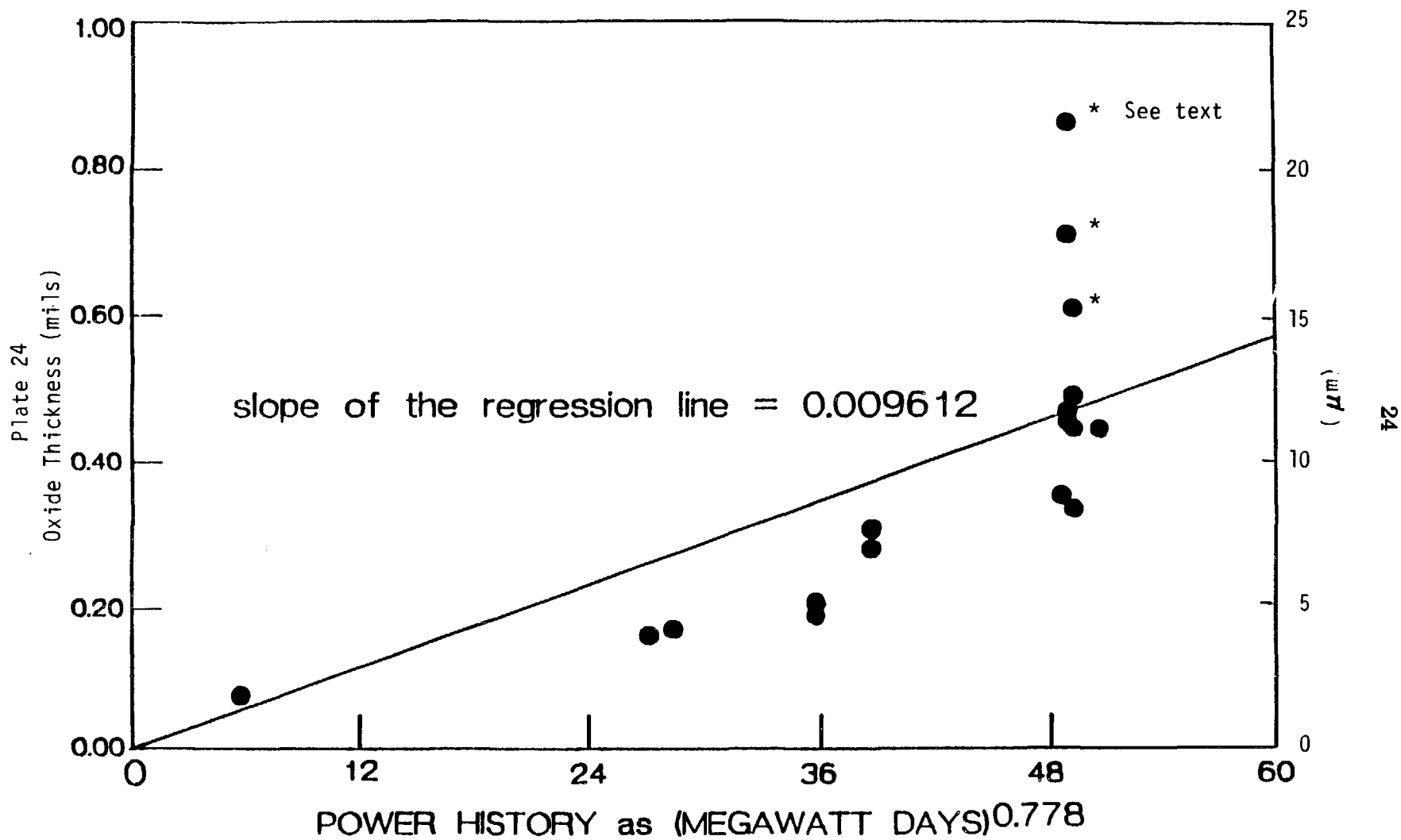


Fig. 11.1. Oxide measurements on 775-g fuel elements.

## 12. SUGGESTIONS FOR ALUMINUM OXIDE RESEARCH

The following suggestions were made during the Workshop; these should be considered by ORNL in evaluation of the aluminum cladding oxide problem.

### 12.1 ANS-ORNL CORROSION LOOP AND ASSOCIATED RESEARCH

#### 12.1.1 Near-Term Program

The relationships between aluminum surface area, stainless steel surface area, and coolant volume of the ANS reactor should be matched in the loop experiment. The workshop participants urged use of the "best water chemistry" achievable before adding controlled substances. For water-chemistry conditions, it is important to make certain that all analytical methods are approved methods. The same relative cleanup rates as planned for ANS should be used in the loop. The reproducibility of corrosion data obtained from the test loop should be established. Based on a water pH of 5.0 and other current water-chemistry parameters, the limits of heat flux for the ANS 14-day cycle should be established. Because preliminary results indicate that the desired ANS requirements may not be achieved, a fuel-plate prefilm similar to that used for the ATR, and perhaps others, should be considered. If ANS requirements are still not achieved, adjustment of the pH or water chemistry should be investigated. The idea that the aluminum corrosion rate will be reduced if the loop water is kept saturated with aluminum oxide should also be investigated.

The next hopes are that (1) a corrosion inhibitor such as iron, carbon, or other corrosion-inhibiting compounds could be found and (2) surface treatments such as coatings or implants could reduce oxidation. During the above studies, the tolerance for spallation should be established. Miscellaneous suggestions that should be mentioned include (1) trying different levels of dissolved and particulate oxides in the coolant and (2) including unheated specimens in the test loop with the heated specimens. If the ANS requirements are still not achieved, an extensive development program will become necessary. Possible candidate alternate aluminum alloys are 8001, 2219, 5052, and 5454.

#### 12.1.2 Long-Term Program

Some topics for study include the following: (1) build at least one more loop, because a significant number of tests will be needed; (2) if hydrogen formation can be measured, optimize corrosion rates based on lowest hydrogen evolution; (3) investigate the solubilities of the various aluminum oxide species as functions of pH and temperature; (4) establish oxide species in the corrosion film; (5) attempt to correlate loop corrosion based on solubilities of oxide species and cleanup rate;

(6) study the effect of coolant temperature and coolant velocity; (7) determine the influence of erosion; (8) study the effect of the ratio of stainless steel surface area to aluminum surface area; (9) determine the extent of damage to the aluminum cladding during oxidation; (10) investigate the effects of reversed coolant flow; and (11) measure oxide thickness on HFIR plates.

## 12.2 GENERAL ALUMINUM CLADDING CORROSION RESEARCH

In general, the Workshop did not identify suggestions for general research that must be accomplished immediately. However, many good ideas, which should be considered promptly, were generated.

### 12.2.1 In-Reactor Research

INEL in-reactor oxide buildup experience has been very different from ex-reactor tests. With good coolant chemistry, during and between operating periods, oxide buildup on ATR and ETR fuel plates reached limiting thicknesses of  $<25 \mu\text{m}$  ( $<1$  mil) and resulted in no spallation. Ex-reactor data have not revealed similar limiting thin oxide thicknesses. A better understanding of these observations is important in applying current ORNL loop data to the ANS reactor. The ORNL loop program should be supplemented with in-reactor tests at conditions approximating those of ANS to obtain oxide buildup rates and identify the species present in the film.

In trying to explain the differences between in-reactor and ex-reactor oxidation rate differences, two theories have been offered. One theory is that the prefilm is important and that the conditions at which the prefilming is done (water chemistry and possibly the water temperature) are very important in conjunction with the strict water chemistry control in the reactor. These things are probably all interrelated. Another theory is that the ratio of exposed aluminum surface to total surface areas and/or system volumes needs to be the same for the out-of-reactor loop as it is in the reactor to obtain results that will be valid for the reactor. The relative flow rate of the chemical water cleanup stream to total volume is also a critical factor as well as overall water chemistry and its strict control.

Preliminary exploratory attempts to measure thermal conductivity of reactor-produced oxide film at INEL indicate that in-reactor thermal conductivity may be markedly lower than the ORNL-Griess value for boehmite,  $2.25 \text{ W/m}\cdot^\circ\text{C}$  ( $1.3 \text{ Btu/h}\cdot\text{ft}\cdot^\circ\text{F}$ ).



### 12.2.2 Ex-Reactor Research

There is a very serious lack of basic understanding of the corrosion mechanisms of aluminum alloys, particularly under heat transfer conditions. Some topics for study include the following: (1) characterization of pre- and postexposure conditions of specimen fuel plates, (2) how corrosion-product oxides change with coolant temperature and time, (3) which oxide species are carried in the recirculation coolant and deposited in the out-of-core cooling circuit, (4) what are the solubilities of different corrosion product species, (5) how recirculating system aluminum oxide inventory changes with operation and between-cycle cleanup operation, (6) comparison of corrosion rates calculated from solubility effects with measured corrosion penetrations, (7) clarification of the water content of aluminum oxide crystals and the solubility of corrosion products as a function of temperature and aging (this will require quantitative removal and characterization of oxide layers), (8) expansion of the Griess correlation to include loop chemistry variables and heat flux, and (9) review of the base data and notebooks of the experiments conducted at ETR/ATR in the 1960s.

## REFERENCES AND BIBLIOGRAPHY

1. J. A. Ayres, *Trip Report - Meeting of the Aluminum Alloy Task Group*, HW-45145, USAEC Hanford Operations Office, June 25, 1956.
2. J. M. Atwood, *Trip Report - Aluminum Alloy Task Group Meeting*, HW-46482, USAEC Hanford Operations Office, Nov. 18, 1956.
3. J. A. Ayres and R. J. Lobsinger, *Report of Meeting - Aluminum Alloy Task Group*, HW-48483, USAEC Hanford Operations Office, Jan. 23, 1957.
4. J. A. Ayres and R. L. Dillion, *Trip Report - Meeting of Aluminum Alloy Task Force*, HW-54410, USAEC Hanford Operations Office, Jan. 8, 1958.
5. J. A. Ayres, *Trip Report - Aluminum Alloy Task Group*, HW-56433, USAEC Hanford Operations Office, June 17, 1958.
6. J. A. Ayres and R. L. Dillion, *Progress Report - September 1957-December 1957, Corrosion of Aluminum in Deionized Water*, HW-53963, Hanford Operations Office, Dec. 6, 1957.
7. J. A. Ayres, R. L. Dillon, and R. J. Lobsinger, *Progress Report - January-June 1958*, HW-56225, USAEC Hanford Operations Office.
8. R. L. Dillon, *Dissolution of Aluminum Oxide as a Regulating Factor in Aqueous Aluminum Corrosion*, HW-61089, USAEC Hanford Operations Office, Aug. 31, 1959.
9. D. R. Dickinson and R. J. Lobsinger, *Effect of Oxide Dissolution and Heat Transfer on the Corrosion of Aluminum Fuel Cladding*, HW-77529, USAEC Hanford Operations Office, Dec. 1963.
10. D. R. Dickinson, *Oxide Dissolution in Aluminum Corrosion*, HW-SA-3319, USAEC Hanford Operations Office, Jan. 14, 1964.
11. S. R. Hatcher and H. K. Rae, "Formation and Control of Turbidity in Aluminum-Water Reactor Systems," *Nucl. Sci. Eng.*, 10, 316-330 (1961).

12. E. Deltombe and M. Pourbaix (Translated by C. Groot), *Corrosion* 14(11), 496t (1958).
13. R. S. Ondrejcin, *A Mechanism for Stress Corrosion Cracking of Stainless Steel in Reactor Systems*, DP-1089, USAEC Savannah River Operations Office, Dec. 1969.
14. J. C. Griess, H. C. Savage, and J. L. English, *Effect of Heat Flux on the Corrosion of Aluminum by Water. Part IV. Tests Relative to the Advanced Test Reactor and Correlation with Previous Results*, ORNL-3541, Union Carbide Corp. Nucl. Division, Oak Ridge Natl. Lab., Feb. 1964.
15. J. C. Griess et al., *Effect of Heat Flux on the Corrosion of Aluminum by Water. Part II. Influence of Water Temperature, Velocity and pH on Corrosion Product Formation*, ORNL-3056, Union Carbide Corp. Nucl. Division, Oak Ridge Natl. Lab., Feb. 10, 1961.
16. J. C. Griess et al., *Effect of Heat Flux on the Corrosion of Aluminum by Water. Part III. Final Report on Tests Relative to the High-Flux Isotope Reactor*, ORNL-3230, Union Carbide Corp. Nucl. Division, Oak Ridge Natl. Lab., Dec. 5, 1961.
17. G. W. Gibson and O. Shupe, *Annual Progress Report on Fuel Element Developments for FY 1961*, IDO-16727, USAEC Idaho Operations Office, March 1962.
18. M. L. Griebenow, G. H. Hanson, M. J. Graber, and D. S. Fjeld, *ANS Transactions*, 14(2), 761 (Oct. 1971).
19. M. L. Griebenow, G. H. Hanson, and A. P. Larrick, *TRA Oxide Film Control and Surveillance (A Reference Document)*, RE-A-77-059, RE&C, Oct. 1977.
20. G. H. Hanson et al., "ATR-ETR Rates of Oxide Film Formation on Aluminum Fuel Plates," *Trans. Am. Nucl. Soc.* 18, 127 (1974).

**Appendix A**  
**WORKSHOP PROGRAM**

# ANS CORROSION WORKSHOP PROPOSED AGENDA

EG&G Idaho, Inc.,  
Willow Creek Bldg., Conference Room No. 1  
Idaho Falls, ID

Wednesday - November 16, 1988

## Session Chairman — Norman Pace

08:30-08:40	Jim Lake, INEL, Welcome
08:40-09:00	Bill Montgomery, ORNL, General ANS Program, Introductory Remarks
09:00-10:00	Dick Pawel, ORNL, ANS Corrosion Tests at ORNL
10:00-10:30	Discussion
10:30-10:45	Break
10:45-11:05	Merle Griebenow, INEL, ATR/ETR Fuel Clad Oxide Assessment
11:05-11:25	Norman Pace, INEL, ATR Oxide Data Base
11:25-11:45	Discussion
11:45-01:00	Lunch

## Session Chairman - Bill Montgomery

1:00-1:30	Bob Dillon, Battelle Northwest, Al Corrosion Experience at Battelle Northwest Labs
1:30-2:00	Discussion

2:00-2:30	Bob Ondrejcin, E.I. DuPont de Nemours, Fuel Clad Corrosion Evaluation at Savannah River Labs
2:30-3:00	Discussion
3:00-3:15	Break
3:15-3:45	John Weeks, BNL, Aluminum Corrosion in HFBR
3:45-4:15	Discussion
4:15-5:00	General discussion

Thursday - November 17, 1988

Session Chairman - Gary Fillmore

08:30-09:00	Charles McKibben, University of Missouri, Observations from University of Missouri Research Reactor
09:00-09:30	Discussion
09:30-10:30	Grady Yoder, ORNL, Some Thoughts on Data Comparisons and Correlations
10:30-10:45	Break
10:45-11:45	Discussion
11:45-1:00	Lunch
	<u>Session Chairman - Grady Yoder</u>
1:00-3:00	Other presentations/discussions
3:00-3:15	Break
3:15-5:00	Reporters discussion and judgements; ANS Clad Oxidation Program directions; wrap-up

**Workshop Reporters:**                    **George Gibson, INEL (retired)**  
   **George Hanson, INEL (retired)**  
   **John Griess, ORNL (retired).**

---

**Note: Points or contributions not made during or immediately following the talks may be accommodated at end-of-day discussion periods. We hope to have a schedule that will encourage exchange of information while maintaining a reasonable degree of order in the proceedings.**

**Appendix B**  
**LIST OF ATTENDEES**



## ANS CORROSION WORKSHOP

## LIST OF ATTENDEES

November 16-17, 1988

Dick Ambrosek  
 Idaho National Engineering  
 Laboratory  
 P.O. Box 1625  
 Idaho Falls, ID 83415-3420  
 (208)526-1247  
 FTS: 583-1247

R. N. Beatty  
 Idaho National Engineering  
 Laboratory  
 P.O. Box 1625  
 Idaho Falls, ID 83415-7129  
 (208)526-4569  
 FTS: 583-4569

Robert Dillon  
 623 Cottonwood  
 Richland, WA 93352  
 (509)946-8113

Ken Farrell  
 Oak Ridge National  
 Laboratory  
 P.O. Box 2008  
 Oak Ridge, TN 37831-6156  
 (615)574-5059

G. N. Fillmore  
 Idaho National Engineering  
 Laboratory  
 P.O. Box 1625  
 Idaho Falls, ID 83415-3420  
 (208)526-1779  
 FTS: 583-1779

George W. Gibson  
 INEL Retired  
 P.O. Box 923  
 Hailey, ID 83333

M. L. Griebenow  
 Idaho National Engineering  
 Laboratory  
 P.O. Box 1625  
 Idaho Falls, ID 83415-3519  
 (208)526-1296  
 FTS: 583-1296

John C. Griess, Jr.  
 10803 Fox Park Road  
 Knoxville, TN 37931

George H. Hanson  
 INEL Retired  
 444 Seventh St.  
 Idaho Falls, ID 83401  
 (208)522-5450

R. R. Hobbins  
 Idaho National Engineering  
 Laboratory  
 P.O. Box 1625  
 Idaho Falls, ID 83415-2506  
 (208)526-9545  
 FTS: 583-9545

R. D. Johnson  
 Idaho National Engineering  
 Laboratory  
 P.O. Box 1625  
 Idaho Falls, ID 83415-7106  
 (208)526-4201  
 FTS: 583-4201

Rod Knight  
 Oak Ridge National Laboratory  
 P.O. Box 2008  
 Oak Ridge, TN 37831-6389  
 (615)574-5713

Jim Lake  
 Idaho National Engineering  
 Laboratory  
 P.O. Box 1625  
 Idaho Falls, ID 83415-3515  
 (208)526-9054  
 FTS: 583-9054

J. Charles McKibben  
 University of Missouri,  
 Research Reactor  
 Research Park  
 Columbia, MO 65211  
 (314)882-5204

Ed McVey  
 Chalk River Nuclear  
 Laboratories Sta 61  
 Atomic Energy of Canada Limited  
 Chalk River, Ontario,  
 CANADA KOJ LJO  
 (613)584-311 ext. 4673

R. L. Miller  
 Idaho National Engineering  
 Laboratory  
 P.O. Box 1625  
 Idaho Falls, ID 83415-2210  
 (208)526-0259  
 FTS: 583-0259

Bill Montgomery  
 Oak Ridge National Laboratory  
 P.O. Box 2008  
 Oak Ridge, TN 37831-8001  
 (615)574-0258

Chang Oh  
 Idaho National Engineering  
 Laboratory  
 P.O. Box 1625  
 Idaho Falls, ID 83415-3515  
 (208)526-9369  
 FTS: 583-9369

Robert S. Ondrejcin  
 E.I. du Pont de Nemours & Co.  
 Savannah River Laboratory  
 Aiken, SC 29808  
 (803)725-3592

Norman E. Pace  
 Idaho National Engineering  
 Laboratory  
 P.O. Box 1625  
 Idaho Falls, ID 83415-3420  
 (208)526-0398  
 FTS: 583-0398

Dick Pawel  
 Oak Ridge National Laboratory  
 P.O. Box 2008  
 Oak Ridge, TN 37831-6156  
 (615)574-5138

John Ryskamp  
 Idaho National Engineering  
 Laboratory  
 P.O. Box 1625  
 Idaho Falls, ID 83415-3515  
 (208)526-9533  
 FTS: 583-9533

K. Vinjamuri  
 Idaho National Engineering  
 Laboratory  
 P.O. Box 1625  
 Idaho Falls, ID 83415-2506  
 (208)526-9277  
 FTS: 583-9277

R. P. Wadkins  
 Idaho National Engineering  
 Laboratory  
 P.O. Box 1625  
 Idaho Falls, ID 83415-3420  
 (208)526-0428

**John Weeks**  
**Brookhaven National Laboratory**  
**Associated Universities, Inc.**  
**Bldg. 130**  
**Upton, Long Island, NY 11973**  
**(516)282-2617**

**Grady Yoder**  
**Oak Ridge National Laboratory**  
**P.O. Box 2008**  
**Oak Ridge, TN 37831-8045**  
**(615)574-5282**

**Patrick Williams**  
**Babcock and Wilcox Co.**  
**NNSD**  
**P.O. Box 785, Mail Code 61**  
**Lynchburg, VA 24505**  
**(804)522-5865**